

INFLUENCE OF CURING-LIGHT BEAM PROFILE NON-UNIFORMITY ON  
DEGREE OF CONVERSION AND MICRO-FLEXURAL STRENGTH  
OF RESIN-MATRIX COMPOSITE

by

Yousef Tariq Eshmawi

Submitted to the Graduate Faculty of the School of  
Dentistry in partial fulfillment of the requirements  
for the degree of Master of Science in Dentistry,  
Indiana University School of Dentistry, April 2017.

Thesis accepted by the faculty of the Department of Operative Dentistry, Indiana University School of Dentistry, in partial fulfillment of the requirements for the degree of Master of Science in Dentistry.

---

Anderson T. Hara

---

Kim E. Diefenderfer

---

Jeffrey A. Platt  
Chair of the Research Committee

---

Norman B. Cook  
Program Director

---

Date

## DEDICATION

This thesis is dedicated to my parents and siblings, for their unlimited support,  
encouragement, inspiration and prayers.

## ACKNOWLEDGMENTS

I would like to express my sincere gratitude to the Royal Government of Saudi Arabia and Umm Al-Qura University for giving me the opportunity to earn my graduate degree.

I would like to express my deepest appreciation to my mentor, Dr. Jeffrey A. Platt, for his encouragement, patience, thoughtful feedback, and guidance, without which this thesis would not have been possible.

I also would like to convey my sincere appreciation to my research committee professors, Drs. Norman B. Cook, Kim E. Diefenderfer and Anderson Hara for their unlimited support and help during my MSD project.

I would like to express my gratitude to Mr. George Eckert for his statistical expertise.

I also would like to show special gratitude to Dr. Li Ding for her assistance in the laboratory.

Finally, there are no adequate words to convey my appreciation to my family and friends for all they have done for me.

## TABLE OF CONTENTS

Introduction.....	1
Review of Literature .....	5
Methods and Materials.....	14
Results.....	20
Tables and Figures .....	24
Discussion.....	46
Summary and Conclusions .....	52
References.....	54
Abstract.....	62
Curriculum Vitae	



## LIST OF ILLUSTRATIONS

TABLE I	Composition of Tetric EvoCeram resin-matrix composite.....	25
TABLE II	Treatment groups and curing locations.....	26
TABLE III	Mean $\pm$ SE of the irradiance ( $\text{mW}/\text{cm}^2$ ) received by the resin-matrix composite using the evaluated LCUs at different locations.....	27
TABLE IV	Mean $\pm$ SE of the radiant exposure ( $\text{J}/\text{cm}^2$ ) received by the resin-matrix composite using the evaluated LCUs at different locations.....	28
TABLE V	Mean $\pm$ SE of DC for the evaluated LCUs at different locations.....	29
TABLE VI	Mean $\pm$ SE for $\mu$ -flexural strength (MPa) for the evaluated LCUs at different locations.....	30
FIGURE 1	Top left: A single emission peak LED LCU (Demi Ultra). Top right: A multiple emission peak LED LCU (VALO Cordless). Bottom: A QTH LCU (Optilux 401).....	31
FIGURE 2	Top: A Managing Accurate Resin Curing System-Resin Calibrator (MARC-RC) system. Bottom: MARC-RC top and bottom sensors.....	32
FIGURE 3	Top: Polyvinyl chloride (PVC) mold. Bottom: The rectangular opening of the PVC mold centered over the 4 mm MARC-RC bottom sensor.....	33
FIGURE 4	Illustration of the RMC packed into the rectangular opening of the mold with a hand instrument.....	34
FIGURE 5	Illustration of the specimen locations where the measurements were collected relative to each light-curing unit (LCU) tip.....	35
FIGURE 6	Illustration of the LED LCU mounted over the top sensor of MARC-RC to measure the amount of irradiance and radiant exposure received by the top surface of RMC specimen.....	36

FIGURE 7	Illustration of the LED LCU mounted over the bottom sensor of MARC-RC and at 0-mm distance between the top of the specimen and the light guide to measure the amount of irradiance and radiant exposure received by the bottom surface of RMC specimen.....	37
FIGURE 8	Illustration of the specimen locations relative to the beam profile of the LCU and superimposed over a Class II cavity preparation at different LCLs.....	38
FIGURE 9	Flowchart of the experimental design. Abbreviations. DC: Degree of conversion. $\mu$ -flexural strength: micro-flexural strength.....	39
FIGURE 10	Illustration of the degree of conversion (DC) measurement locations on the top and bottom surfaces of a RMC specimen.....	40
FIGURE 11	Illustration of $\mu$ -flexural strength test setup.....	41
FIGURE 12	Mean $\pm$ SE of the irradiance ( $\text{mW}/\text{cm}^2$ ) for the evaluated LCUs at different locations.....	42
FIGURE 13	Mean $\pm$ SE of the radiant exposure ( $\text{J}/\text{cm}^2$ ) for the evaluated LCUs at different locations.....	43
FIGURE 14	Mean $\pm$ SE of degree of conversion for the evaluated LCUs at different locations.....	44
FIGURE 15	Mean $\pm$ SE of $\mu$ -flexural strength (MPa) for the evaluated LCUs at different locations.....	45

## INTRODUCTION

An estimated 260 million resin-matrix composite (RMC) restorations are placed annually around the world.<sup>1</sup> A recent Cochrane Systematic Review revealed that the failure rate of posterior RMC restorations was twice that of posterior amalgam restorations.<sup>2</sup> Also, the median longevity of posterior RMC restorations was six years,<sup>3-5</sup> with bulk fracture and secondary caries the most common causes of failure.<sup>2,4,6,7</sup>

The degree of conversion (DC) has a significant impact on the performance of RMC restorations. It was found that DC is positively correlated with increasing the amount of radiant exposure received by RMC.<sup>8</sup> Conversely, unreacted monomers may plasticize the polymer structure, degrading the mechanical properties of RMC restorations.<sup>9,10</sup>

The irradiance can be defined as the radiant power per surface of known dimensions ( $\text{mW}/\text{cm}^2$ ). However, the radiant exposure is the total amount of energy delivered to a resin-matrix composite surface during the entire irradiation procedure ( $\text{J}/\text{cm}^2$ ).<sup>11</sup>

Previous studies have investigated the wavelength distribution and light intensity of light curing units (LCUs) and found that many light emitting diode (LED) LCUs do not deliver their intended light output.<sup>12-14</sup> In addition, the off-center position of the LED chips of some multiple emission peak LED LCUs may affect the beam profile uniformity.<sup>15-17</sup> Therefore, several laboratory studies have examined the light beam profile uniformity of different LCUs and revealed that the irradiance ( $\text{mW}/\text{cm}^2$ ) and

spectral emission (nm) distribution were non-uniform across the LCU tip and may result in non-uniform polymerization of RMC restoration.<sup>11,11,15-20</sup> This may negatively affect the properties and longevity of the restoration.<sup>16-18, 21-23</sup> A clinical study reported a direct correlation between insufficient light exposure and decreased wear resistance of RMC.<sup>24</sup> Additionally, a direct relation was found between irradiance and the rate of free radical production.<sup>25</sup> Thus, appropriate irradiance and spectral emission delivered from the LCUs is required to obtain an optimum number of free radicals and achieve adequate polymerization of a RMC.<sup>19,26-28</sup>

Material properties, such as fracture resistance and elasticity, are often evaluated by flexural strength, flexural modulus and fracture toughness.<sup>29</sup> The flexural strength test is performed to predict the mechanical behavior of RMC because it resembles the compressive and tensile forces that are exerted in the stress concentration area and around the point of loading.<sup>30</sup> Additionally, it was reported that appropriate curing of RMC could improve the material's flexural properties.<sup>31,32</sup>

Several previous studies have evaluated  $\mu$ -flexural strength of dental adhesive systems<sup>33-35</sup> using RMC specimens of smaller dimensions than suggested in the ISO 4049 flexural strength standard.<sup>32,36,37</sup>

The aim of this study was to evaluate the effect of the beam profile of a single and multiple emission peak LED LCU on the DC and  $\mu$ -flexural strength at different light curing locations (LCLs) compared with quartz tungsten halogen (QTH) LCU.

## HYPOTHESES

### Null Hypothesis

Changing the horizontal location of LED LCUs will have no significant effect on the DC and micro-flexural strength of RMC compared with a QTH LCU.

### Alternative Hypothesis

Changing the horizontal location of LED LCUs will have a significant effect on the DC and micro-flexural strength of RMC compared with a QTH LCU.

## REVIEW OF LITERATURE



The development of LCUs allowed for the curing on demand of dental restorative materials.<sup>26</sup> Even though they have brought this advantage to dentistry, many issues associated with LCUs exist, such as confusion about adequacy of irradiance, radiant exposure, and exposure duration that may affect the polymerization of RMC.<sup>26,38</sup>

#### LIGHT CURING BEAM PROFILE NON-UNIFORMITY

Light beam non-uniformity has been significantly associated with the introduction of the LED LCUs and is caused by non-uniform distribution of spectral emission across the LCU tip.<sup>20</sup> Similar discrepancies were detected with ultraviolet (UV) and visible LCUs in 1983 and 1985, respectively.<sup>39,40</sup> It was proposed that moving the LCU tip during photoinitiation might result in a more uniform polymerization of RMC restorations.<sup>41</sup> However, it was found that circular motion of the LCU tip resulted in non-uniform distribution of the hardness values across RMC specimens.<sup>42</sup>

Several methods are available to measure the light output of LCUs.<sup>15,43</sup> Of these, the light beam analyzer can accurately evaluate the power distribution across the LCU tip by taking a snapshot of the light source. Then, the average power value can be calculated at a specific area in the light beam. This value is termed the top hat factor, which represents the uniformity of the power distribution across the LCU tip.<sup>44,45</sup>

In 2010 Price et al.<sup>46</sup> evaluated the effect of using different light guides on the irradiance distribution and uniformity from different LCUs. They showed that the irradiance was non-uniform across the LCU tip and it differed significantly among the

LCU products and the types of light-generating methods. Furthermore, the light beam non-uniformity varied greatly when using different light guides on the same LED LCU body. Also, the authors concluded that a single irradiance value does not reflect the differences in irradiance across the LCU tip when characterizing a specific LCU. In addition, the irradiance distribution, the overall irradiance, and the top hat factor are significant factors that should be included when describing the irradiance of LCUs.<sup>46</sup>

Some LCUs with a broad spectral emission such as QTH and plasma arc (PAC) may not show significant differences in the wavelength distribution across the light beam.<sup>16,20</sup> On the other hand, due to the off center position of the chips in LED LCUs, the wavelength distribution can be non-uniform across the LCU tip.<sup>24</sup>

Price et al.<sup>21</sup> evaluated the irradiance uniformity across the LCU tips of multiple emission peak LED LCUs at two different spectral emission wavelengths. A significant difference was found in the irradiance uniformity between 405 nm and 460 nm wavelengths, which is mainly dependent on the location of the LED chips and their emission wavelengths within the LCU. Also, the authors suggested that the spectral radiant power should be included to characterize the light output along with the top hat factor and the irradiance distribution.<sup>21</sup>

In 2014 Michaud et al.<sup>16</sup> also evaluated the localized irradiance and wavelength distributions of four LCUs, one PAC, one single emission peak, and two multiple emission peak LED LCUs. The irradiance was found to be non-uniform with all LCUs. However, a PAC LCU had the most uniform irradiance distribution across the LCU tip, while the most non-uniform irradiance and spectral emission distribution occurred with multiple emission peak LED LCUs. The authors also concluded that the irradiance and

spectral emission of LCUs should not be reported as a single value as it will not precisely describe the output of the LCUs. Instead, they recommended providing an image to illustrate the irradiance and spectral emission distribution across the LCU tip.<sup>16</sup>

Price et al.<sup>19</sup> also investigated the effect of distance on the irradiance and light beam uniformity of four LED LCUs. In this study, the irradiance at the center of the light beam was measured at 1 mm and 9 mm distances between the LCU tip and a 3.9-mm diameter irradiance probe. The light beam uniformity was determined by calculating the mean top hat factor (measured at 2-, 4-, 6-, and 8-mm distances from the LCU tip). The light beam uniformity, the irradiance at the center of the light beam, and the top hat factor varied significantly among all LCUs. Therefore, the authors concluded that 1) Increased distance between the LCU and RMC might result in suboptimal polymerization, specifically with deep restorations, and (2) The light output cannot be represented by a single irradiance value.<sup>19</sup>

In 2014 Megremis et al.<sup>20</sup> investigated seven LED LCUs and included a QTH LCU as a reference point for all the tests. In this study, the irradiance, spectral distribution and the light beam uniformity were evaluated. The irradiance distribution of all LED LCUs was non-uniform across the LCU tip relative to the QTH LCU and it was recommended that clinicians should consider the location of the high irradiance regions on the LCU tip relative to the size of RMC restoration. Also, the position of the LCUs might significantly influence the radiant power and the wavelength received by RMC restorations.

A few studies have evaluated the effect of the light curing beam profile non-uniformity on DC and RMC physical properties.<sup>15,17,18,23,44</sup> However, no studies (*in vivo*

or *in vitro*) were found to evaluate the effect of the light beam non-uniformity on the mechanical properties of RMC restorations. In 2005 Vandewalle et al.<sup>44</sup> evaluated the influence of the light dispersion of QTH and LED LCUs on the DC of RMC. In this study, the DC was significantly influenced by the divergence angle of the light beam emitted from LCUs, as the lower the light dispersion, the higher the polymerization of RMC at greater distances. However, the DC values with LED LCUs were found to be either similar or better compared to QTH LCU at 5-mm distance between RMC and the LCU tip. Similarly, Arikawa et al.<sup>15</sup> measured the effect of light beam profile non-uniformity on RMC surface hardness. In this study, three QTH, one PAC, and one LED LCU were investigated. The light intensity varied significantly among all LCUs at different locations across the LCU tip. However, for all LCUs, the distribution patterns of the surface hardness corresponded roughly with light intensity. Also, compared to LED, QTH and PAC showed significantly greater non-uniformity in light intensity distribution. Furthermore, increasing the distance between the light guide tip and RMC specimens did not effectively compensate for the light beam non-uniformity of LCUs. Additionally, for all LCUs, increased light beam non-uniformity significantly reduced the surface hardness of RMC specimens.

In 2008 Vandewalle et al.<sup>18</sup> assessed the effect of the light guide type on the distribution of irradiant emission from an LED LCU and evaluated the effect of the light dispersion on surface hardness of two types of RMC. In this study, the authors found a more uniform light distribution when using the standard guide than the turbo guide. Also, higher hardness values were found at higher irradiance locations on both top and bottom surfaces.

More recently, Price et al.<sup>17</sup> correlated the effects of irradiance and spectral emission inhomogeneities of a multiple emission peak LED LCU on the microhardness of RMC containing either camphorquinone (CQ) or a combination of CQ and trimethylbenzoyl-diphenylphosphine oxide (TPO) photoinitiator systems. In general, the irradiance and spectral emission were non-uniform across the LCU tip. However, the authors found a significant positive correlation between the irradiance beam profile and the microhardness values for RMC specimens cured for 5 seconds and 10 seconds. This correlation increased with RMC specimens containing both CQ and TPO photoinitiators and decreased with increasing curing time for RMC specimens containing CQ only. Haenel et al.<sup>23</sup> also investigated the effect of irradiance distribution of multiple emission peak and single emission peak LED LCUs on the microhardness of RMC. RMC hardness values correlated significantly with the irradiance distribution across the LCU tip.

Total radiant exposure is the product of irradiance and exposure time. Comparable material properties may result from similar radiant exposure regardless of how it was obtained (amount of irradiance, exposure time). This principle is known as the “exposure reciprocity law.”<sup>47</sup> Price et al.<sup>11</sup> suggested that increasing the light curing time beyond the manufacturer recommendations might partially overcome the effect of light beam non-uniformity on the polymerization and microhardness of RMC.<sup>11</sup> However, Haenel et al.<sup>23</sup> found that extending the exposure time did not compensate for the effect of the light beam non-uniformity on the microhardness of RMC specimens, which confirms the findings of previous reports on exposure reciprocity.<sup>47-49</sup>

## DEGREE OF CONVERSION AND FLEXURAL STRENGTH

Adequate polymerization of RMC is an essential requirement for long and predictable clinical performance.<sup>38,50-52</sup> Previous studies have evaluated the DC and flexural strength of different restorative materials to predict their clinical performance when subjected to mastication stresses after being introduced to the oral environment. Ferracane et al.<sup>53</sup> in 1985 found a significant positive correlation between increasing DC and microhardness values of RMC specimens.<sup>53</sup> Likewise, in 2003 Palin et al.<sup>31</sup> evaluated the DC and flexural strength of several RMC materials and found that lower DC values could significantly compromise the flexural strength properties of RMC.

RMC materials will attain their maximum physical and mechanical properties only if they receive adequate energy at an appropriate wavelength.<sup>20</sup> In 2006 Calheiros et al.<sup>32</sup> reported that increasing the radiant exposure could positively affect the flexural strength but not necessarily the DC of RMC. However, the authors emphasized the consequences of increasing the photoactivation of RMC, as it may result in temperature rise of the surrounding tissues.<sup>32</sup> Gonzalez et al.<sup>54</sup> investigated the effect of the irradiance and radiant exposure on the DC and the mechanical properties of two different RMC materials. Higher irradiance values significantly improved the flexural strength properties but did not influence the DC of RMC. Therefore, from the previous studies, it can be concluded that the flexural properties were found to be improving with adequate polymerization of RMC.<sup>31,32, 54,55</sup> However, the DC and flexural strength of RMC were also found to be significantly influenced by the material composition, as increasing the monomer concentration, viscosity and opaque filler loading could significantly decrease the DC of RMC. Also, the amount of the filler content of RMC could be influenced by

the filler morphology and may affect the flexural strength of RMC.<sup>56-59</sup>

## ISOTROPIC AND ANISOTROPIC BEHAVIOR OF RMC

Polymers could have either completely non-crystalline (amorphous) or semi-crystalline structure.<sup>60</sup> However, several factors could affect the crystallinity of the polymer structure. Among those factors are the symmetry, intermolecular bonding, tacticity, molar mass, and branching of the polymer chain.<sup>60</sup> Linear chains with symmetrical units increase the ability of a polymer to crystallize.<sup>60</sup> Also, polymer chains that have large pendant groups will increase the rigidity and result in the difficulty to form a crystalline array.<sup>60</sup> Additionally, if the chain is significantly branched, the packing efficiency deteriorates and the crystalline content is lowered.<sup>60</sup> The crystallographic direction of a crystalline material is defined as a line between two atoms or a vector in the material crystal structure. The physical properties of some crystalline materials may depend on their crystallographic direction. For example the elastic modulus of a material may vary according to the atomic direction in its crystal structure, which means that the material may behave differently when subjected to forces in different directions.<sup>61</sup> The directionality of the properties is termed anisotropy.<sup>61</sup> However, materials with properties independent of their atomic direction are termed isotropic.<sup>61</sup> RMC with particulate fillers such as restorative and veneering composite is considered to have isotropic behavior because of its randomly oriented fillers. Thus, its properties are the same in all directions.<sup>61</sup> On the other hand, resin-impregnated fiber-reinforced composites were introduced to improve the mechanical and esthetic properties of RMC restorations.<sup>62-64</sup> However, the mechanical properties of fiber-reinforced composite may vary significantly according to the orientation of the fibers, as unidirectional fiber orientation produces

anisotropic properties, whereas randomly oriented fibers gives isotropic properties.<sup>65</sup>

In 2003 Dyer et al.<sup>66</sup> evaluated the influence of fiber position and orientation on fracture load of fiber-reinforced RMC using a three-point loading test. Both the orientation and the position of the fibers significantly influenced the fracture load to initial and final failure, as unidirectional glass fibers located on the tension side showed significantly higher fracture load values compared with fibers with diagonal orientation on the compression side.<sup>66</sup> Therefore, it is necessary to consider the type, the orientation, and the position of the fillers used in RMC, as they may affect the fracture load of RMC.



## MATERIALS AND METHODS

## MATERIALS

A quartz-tungsten-halogen (QTH) LCU (Optilux 401, Kerr, Orange, CA) (O), a multiple emission peak LED LCU (VALO Cordless, Ultradent, South Jordan, UT) (V) and a single emission peak LED LCU (Demi Ultra, Kerr, Orange, CA) (DU) were investigated (Figure 1). The diameters of the light guides for O, V and DU were 11 mm, 10 mm and 8 mm, respectively. A nano-hybrid resin-matrix composite, Tetric EvoCeram, (Bleaching shade XL, Ivoclar Vivadent, Amherst, NY) with a total inorganic filler content of 60% to 61% (by volume) and CQ and TPO photoinitiators was used in this study (Table I).

A Managing Accurate Resin Curing System-Resin Calibrator (MARC-RC) system (Bluelight Analytics Inc., Halifax, Canada) was used to monitor the amount, type, and rate of energy delivered to the top and bottom surfaces of RMC specimens (Figure 2).<sup>67</sup> The MARC-RC contains a National Institute of Standards and Technology (NIST)-referenced miniature spectrometer (USB4000, Ocean Optics, Dunedin, FL) with a 3,648-element linear CCD array detector (TCD1304AP, Toshiba, Tokyo, Japan).<sup>68</sup> The sensor is a CC3 cosine corrector (4-mm diameter) designed to collect radiation higher than a field of view of 180°, eliminating optical interface problems associated with the light collection sampling geometry.<sup>68</sup>

## SAMPLE PREPARATION

The specimens were prepared in a constant temperature room (21°C) with 380-nm to 520-nm filtered ambient light.

Forty-five specimens were prepared and assigned to nine groups ( $n = 5$ ) according to their light curing locations (LCLs) (1, 2, 3) (Table II) using a custom-made dark polyvinyl chloride (PVC) mold. The mold was designed with a rectangular opening centered over the 4-mm MARC-RC bottom sensor and an external shape that fit into the well of the bottom sensor to prevent mold rotation and to standardize the location of the specimens relative to each LCU (Figure 3). To analyze the effect of the beam profile of the LCUs on  $\mu$ -flexural strength, rectangular RMC specimens were made with dimensions (2-mm width  $\times$  1-mm thickness  $\times$  6-mm length) allowing them to be polymerized in one exposure. The mold was placed on a Mylar strip and on top of a microscope slide. Then, Tetric EvoCeram bleaching shade XL was packed into the rectangular opening of the mold with a hand instrument and covered with another Mylar strip and a microscope slide to compress the excess resin (Figure 4). The mold with Mylar strips only was placed on the bottom sensor of MARC-RC. The light beam profile of each LCU was previously quantified using a beam profiler system combined with mean power measurements calculated from the irradiance values collected from a MARC-RC system (Figure 5).<sup>69</sup> Each LCU was mounted on a mechanical arm perpendicular to and centered over the top sensor of MARC-RC, and the irradiance and radiant exposure for each LCU were collected at three different LCLs: 1) at the center of the end of the tip; 2) at 1.5 mm to the left of the center of the end of the tip; and 3) at 1.5 mm to the right of the center of the end of the tip (Figure 6). Then, the LCU was shifted

over the bottom sensor without changing the alignment of the LCU (Figure 7). Each LCU was mounted to be parallel to the RMC specimens and at 0-mm distance between the top of the specimens and the light guide tip. For each LCU, specimens were polymerized for 10 seconds according to manufacturer recommendations (Figure 8), and the amount of irradiance and radiant exposure transmitted through the specimen were estimated during the photoactivation of each specimen. To simulate a clinical situation, RMC specimens were photoactivated from the top surface only. After that, the specimens were removed from the mold and placed in a well-plate containing deionized (DI) water and covered with aluminum foil to prevent light from reaching the specimen (Figure 9).

#### FINISHING AND POLISHING

Immediately after fabrication, specimens were mounted over a circular block and stabilized with molten wax applied around each specimen and the block was placed on the finishing and polishing machine. Specimens were finished using a Struers RotoForce-4 polishing unit (Struers, Ballerup, Denmark) using 1,200-, 2400- and 4,000-grit SiC abrasive paper for 1 second, 8 seconds, and 19 seconds respectively and with 5 N force on each specimen. Then, specimens were polished using 1- $\mu$ m diamond polishing suspension (Struers, Ballerup, Denmark) and ultrasonically cleaned for 20 min in DI water. Specimens were stored wet in DI water at 37°C for 24 hours.

#### DEGREE OF CONVERSION (DC)

An Attenuated Total Reflectance-Fourier Transform Infrared (ATR-FTIR) spectrometer (ATR-MIRacle, Pike Technologies, Madison, WI, and JASCO 4100 International Co., Tokyo, Japan) was used to measure the DC. The ATR had a 1.8-mm

diameter diamond crystal plate. Uncured RMC specimens were measured ( $n = 3$ ). The area under the  $1608\text{ cm}^{-1}$  peak was assigned to the aromatic C=C, and the area under the  $1637.5\text{ cm}^{-1}$  peak was assigned to the vinyl C=C.<sup>35,37, 38,56</sup> Cured RMC specimens were placed over the crystal and secured with a swivel pressure clamp to ensure adaptation. The absorbance was measured using 64 scans and  $4\text{ cm}^{-1}$  resolution. Three measurements were obtained from different locations (A, B, C) on the top and bottom surface of each specimen (Figure 10). The average of the three measurements on the top surface was compared with the average of the three measurements on the bottom. The DC was calculated using the following equation<sup>70</sup>:

$$\text{Degree of conversion} = \left(1 - \frac{\text{cured (area under 1637.5/area under 1608)}}{\text{uncured (area under 1637.5/area under 1608)}}\right) \times 100$$

#### MICRO-FLEXURAL STRENGTH ( $\mu$ -flexural strength)

Twenty-four hours after specimen preparation, a micro-three-point bending test using a universal mechanical testing machine (MTS, Eden Prairie, MN) at a crosshead speed of  $1\text{ mm/min}$  with support span of  $4\text{ mm}$  was used to determine  $\mu$ -flexural strength (Figure 11). Flexural strength ( $\sigma$ ) was calculated in megapascals (MPa) using the following equation:

$$\sigma = \frac{3Fl}{2bh^2}$$

Where ( $F$ ) was the maximum load exerted on the specimens in Newtons; ( $l$ ) was the distance between the supports in mm; ( $b$ ) was the width of the specimen in mm; ( $h$ ) was the height of the specimen in mm.

## STATISTICAL ANALYSIS

Irradiance, radiant exposure, and DC were analyzed using three-way ANOVA, with each LCU-LCL-surface combination allowed to have a different variance, and random effects to correlate multiple measurements from each specimen. The  $\mu$ -flexural strength was analyzed using two-way ANOVA, with each LCU-LCL combination allowed to have a different variance. A 5-percent significance level was used for all tests.

## RESULTS

## IRRADIANCE AND RADIANT EXPOSURE

Tables III and IV, Figure 12 and Figure 13 demonstrate mean  $\pm$ SE of the irradiance and radiant exposure for the evaluated LCUs at different LCLs. The bottom surface of a RMC specimen received significantly lower irradiance and radiant exposure compared with the top, regardless of the LCL ( $p < 0.0001$ ). Comparing the irradiance received on a RMC specimen, LCL 1 received significantly higher irradiance than LCL 2 for top using DU ( $p = 0.0033$ ) and V, regardless of the surface ( $p = 0.0008$ ). LCL 1 received significantly higher irradiance than LCL 3 for top using DU ( $p = 0.0045$ ) and V ( $p = 0.0081$ ). LCL 2 received significantly higher irradiance than LCL 3 using DU regardless of the surface ( $p = 0.0382$ ) and bottom using O ( $p = 0.0153$ ). However, LCL 2 received significantly lower irradiance than LCL 3 for bottom using V ( $p = 0.0024$ ). Comparing the LCUs, DU delivered significantly higher irradiance than O ( $p < 0.0001$ ) and V ( $p < 0.0001$ ). Also, V delivered significantly higher irradiance than O ( $p < 0.0001$ ).

Comparing the radiant exposure, LCL 1 received significantly higher radiant exposure than LCL 2 for top using DU ( $p = 0.0001$ ) and V, regardless of the surface ( $p = 0.0009$ ), and significantly lower radiant exposure than LCL 2 for bottom using O ( $p = 0.0333$ ). LCL 1 received significantly higher radiant exposure than LCL 3 for top using DU ( $p = 0.0008$ ) and V ( $p = 0.0176$ ). LCL 2 received significantly higher radiant exposure than LCL 3 for bottom using O ( $p = 0.00383$ ). However, lower radiant exposure was received at LCL 2 than LCL 3 for top using DU ( $p = 0.0175$ ) and bottom using V ( $p$



= 0.0004). Comparing the LCUs, DU delivered significantly higher radiant exposure than O ( $p < 0.0001$ ) and V ( $p < 0.0001$ ), and V was significantly higher than O ( $p < 0.0001$ ).

#### DEGREE OF CONVERSION (DC)

Table V and Figure 14 demonstrate the mean  $\pm$ SE of DC for the evaluated LCUs at different LCLs. The bottom had significantly higher DC than the top for DU in LCL 1 ( $p = 0.0113$ ). However, the bottom was significantly lower than the top at LCL 2 ( $p = 0.0042$ ). Also, the bottom was significantly lower than the top for O regardless of LCL ( $p = 0.0005$ ). And the bottom was significantly lower than the top for V at LCLs 2 and 3 ( $p = 0.0001$ ). LCL 1 was significantly lower than 2 and 3 for the top of DU and V ( $p < 0.0020$ ). The bottom of DU was significantly higher than O in all LCLs ( $p = 0.0039$ ). Furthermore, DU was significantly higher than O on the top at LCL 2 ( $p = 0.0017$ ). However, DU was significantly lower for the top at LCL 1 than O ( $p = 0.0036$ ). DU was significantly higher than V for the bottom in all LCLs ( $p = 0.0001$ ). O was significantly higher than V for top at LCL 1 ( $p = 0.0004$ ) but was significantly lower at LCL 2 ( $p = 0.0258$ ).

#### MICRO-FLEXURAL STRENGTH ( $\mu$ -flexural strength)

Table VI and Figure 15 demonstrate the mean  $\pm$ SE for  $\mu$ -flexural strength (MPa) for the evaluated LCUs at different LCLs. DU was significantly lower than O ( $p < 0.0450$ ) and V ( $p < 0.0250$ ) for LCLs 1 and 3. However, LCL 1 was significantly lower than 2 for DU ( $p = 0.0476$ ).

In general, locations that received higher irradiance exhibited higher radiant exposure values, but did not necessarily show higher DC or flexural strength values. In

addition, the DC values did not seem to influence the flexural strength of RMC specimens.

## TABLES AND FIGURES

TABLE I

Composition of Tetric EvoCeram resin-matrix composite

<b>Composition</b>	<b>Weight (%)</b>
Bis-GMA, Urethane dimethacrylate, Ethoxylated Bis-EMA	16.8
Barium glass filler, Ytterbium trifluoride, Mixed oxide	48.5
Prepolymers	34.0
Additives	0.4
Catalysts and Stabilizers	0.3
Pigments	<0.1
Camphorquinone (CQ), trimethylbenzoyl diphenylphosphine oxide (TPO) photoinitiators	

TABLE II

Treatment groups and curing locations.

<b>Group (Location)</b>	<b>Light curing unit</b>	<b>Light curing tip location (mm)</b>	<b>N</b>
1	Multiple emission	Center	5
2	peak LED	1.5 mm to the left	5
3	VALO Cordless (Test)	1.5 mm to the right	5
1	Single emission peak	Center	5
2	LED	1.5 mm to the left	5
3	Demi Ultra (Test)	1.5 mm to the right	5
1	QTH	Center	5
2	Optilux-401	1.5 mm to the left	5
3	(Control)	1.5 mm to the right	5

TABLE III

Mean  $\pm$ SE of the irradiance ( $\text{mW}/\text{cm}^2$ ) received by the resin-matrix composite using the evaluated LCUs at different locations\*

Mean (SE) irradiance (mW/cm <sup>2</sup> )				
Light Curing Location				
LCU	Surface	1	2	3
Single emission peak				
LED				
Demi Ultra <sup>α</sup>	Top <sup>a</sup>	1336.9 (3.3) <sup>A</sup>	1301.7 (1.4) <sup>B</sup>	1296.8 (0.8) <sup>C</sup>
	Bottom <sup>b</sup>	86.5 (2.0) <sup>AB</sup>	89.1 (2.2) <sup>A</sup>	86.7 (1.1) <sup>B</sup>
QTH				
Optilux <sup>γ</sup>	Top <sup>a</sup>	800.4 (9.8) <sup>A</sup>	850.6 (16.7) <sup>A</sup>	837.9 (13.0) <sup>A</sup>
	Bottom <sup>b</sup>	42.9 (0.4) <sup>AB</sup>	45.8 (1.0) <sup>A</sup>	41.5 (1.0) <sup>B</sup>
Multiple emission peak				
LED				
Valo <sup>β</sup>	Top <sup>a</sup>	1314.0 (2.2) <sup>A</sup>	1279.7 (4.1) <sup>B</sup>	1276.7 (4.9) <sup>B</sup>
	Bottom <sup>b</sup>	62.1 (1.4) <sup>A</sup>	53.4 (1.5) <sup>B</sup>	63.0 (0.4) <sup>A</sup>

\*Superscript lowercase letters represent statistical groups between top and bottom surfaces. Superscript uppercase letters represent statistical groups in the same row. Superscript Greek letters represent statistical groups between LCUs. Abbreviations: Location 1: The center of the end of the tip. Location 2: LCU moved 1.5 mm to the left of the center of the end of the tip. Location 3: LCU moved 1.5 mm to the right of the center of the end of the tip.

TABLE IV

Mean  $\pm$ SE of the radiant exposure ( $\text{J}/\text{cm}^2$ ) received by the resin-matrix composite using the evaluated LCUs at different locations\*

Mean (SE) radiant exposure ( $\text{J}/\text{cm}^2$ )				
Light Curing Location				
LCU	Surface	1	2	3
<b>Single emission peak</b>				
<b>LED</b>				
<b>Demi Ultra<sup>a</sup></b>	Top <sup>a</sup>	13.576 (0.025) <sup>A</sup>	13.267 (0.002) <sup>C</sup>	13.374 (0.032) <sup>B</sup>
	Bottom <sup>b</sup>	0.871 (0.021) <sup>A</sup>	0.909 (0.023) <sup>A</sup>	0.883 (0.012) <sup>A</sup>
<b>QTH</b>				
<b>Optilux-401<sup>b</sup></b>	Top <sup>a</sup>	8.206 (0.142) <sup>A</sup>	8.728 (0.199) <sup>A</sup>	8.633 (0.210) <sup>A</sup>
	Bottom <sup>b</sup>	0.417 (0.005) <sup>B</sup>	0.448 (0.011) <sup>A</sup>	0.402 (0.010) <sup>B</sup>
<b>Multiple emission peak</b>				
<b>LED</b>				
<b>VALO<sup>γ</sup></b>	Top <sup>a</sup>	13.337 (0.001) <sup>A</sup>	13.246 (0.029) <sup>B</sup>	13.240 (0.022) <sup>B</sup>
	Bottom <sup>b</sup>	0.609 (0.018) <sup>A</sup>	0.541 (0.016) <sup>C</sup>	0.638 (0.005) <sup>B</sup>

Superscript lowercase letters represent statistical groups between top and bottom surfaces. Superscript uppercase letters represent statistical groups in the same row. Superscript Greek letters represent statistical groups between LCUs. Abbreviations: Location 1: The center of the end of the tip. Location 2: LCU moved 1.5 mm to the left of the center of the end of the tip. Location 3: LCU moved 1.5 mm to the right of the center of the end of the tip.

TABLE V

Mean  $\pm$ SE of degree of conversion for the evaluated LCUs at different locations.

Mean (SE) degree of conversion				
Light Curing Location				
LCU	Surface	1	2	3
<b>Single emission peak</b>				
<b>LED</b>				
<b>Demi Ultra</b>	Top	54.3 (3.0) <sup>bB<math>\beta</math></sup>	65.8 (2.0) <sup>aA<math>\alpha</math></sup>	62.3 (1.1) <sup>aA<math>\alpha</math></sup>
	Bottom	60.7 (2.7) <sup>aA<math>\alpha</math></sup>	57.5 (1.9) <sup>bA<math>\alpha</math></sup>	58.5 (2.2) <sup>aA<math>\alpha</math></sup>
<b>QTH</b>				
<b>Optilux-401</b>	Top	61.5 (0.8) <sup>aA<math>\alpha</math></sup>	57.6 (0.4) <sup>aA<math>\beta</math></sup>	57.8 (2.3) <sup>aA<math>\alpha</math></sup>
	Bottom	55.2 (1.2) <sup>bA<math>\beta</math></sup>	52.9 (1.9) <sup>bA<math>\beta</math></sup>	52.3 (2.6) <sup>bA<math>\beta</math></sup>
<b>Multiple emission peak</b>				
<b>LED</b>				
<b>VALO</b>	Top	52.0 (0.6) <sup>aB<math>\beta</math></sup>	63.0 (1.3) <sup>aA<math>\alpha</math></sup>	60.6 (1.8) <sup>aA<math>\alpha</math></sup>
	Bottom	52.4 (2.4) <sup>aA<math>\beta</math></sup>	50.5 (2.4) <sup>bA<math>\beta</math></sup>	49.7 (1.5) <sup>bA<math>\beta</math></sup>

\*Superscript lowercase letters represent statistical groups between top and bottom surfaces for each LCU. Superscript uppercase letters represent statistical groups in the same row. Superscript Greek letters represent statistical groups between LCUs for each surface. Abbreviations: Location 1: The center of the end of the tip. Location 2: LCU moved 1.5 mm to the left of the center of the end of the tip. Location 3: LCU moved 1.5 mm to the right of the center of the end of the tip.



TABLE VI

Mean  $\pm$ SE for  $\mu$ -flexural strength (MPa) for the evaluated LCUs at different locations\*

Mean (SE) $\mu$ -flexural strength (MPa) Light Curing Location			
LCU	1	2	3
<b>Single emission peak LED</b>			
<b>Demi Ultra</b>	313 (31) <sup>bB</sup>	400 (13) <sup>aA</sup>	369 (10) <sup>bAB</sup>
<b>QTH</b>			
<b>Optilux-401</b>	401 (12) <sup>aA</sup>	425 (16) <sup>aA</sup>	405 (2) <sup>aA</sup>
<b>Multiple emission peak LED</b>			
<b>VALO</b>	417 (13) <sup>aA</sup>	418 (5) <sup>aA</sup>	458 (21) <sup>aA</sup>

\*Superscript lowercase letters represent statistical groups in the same column. Superscript uppercase letters represent statistical groups in the same row. Abbreviations: 1: The center of the end of the tip. Location 2: LCU moved 1.5 mm to the left of the center of the end of the tip. Location 3: LCU moved 1.5 mm to the right of the center of the end of the tip.



FIGURE 1. Top left: A single emission peak LED LCU (Demi Ultra). Top right: A multiple emission peak LED LCU (VALO Cordless). Bottom: A QTH LCU (Optilux-401).

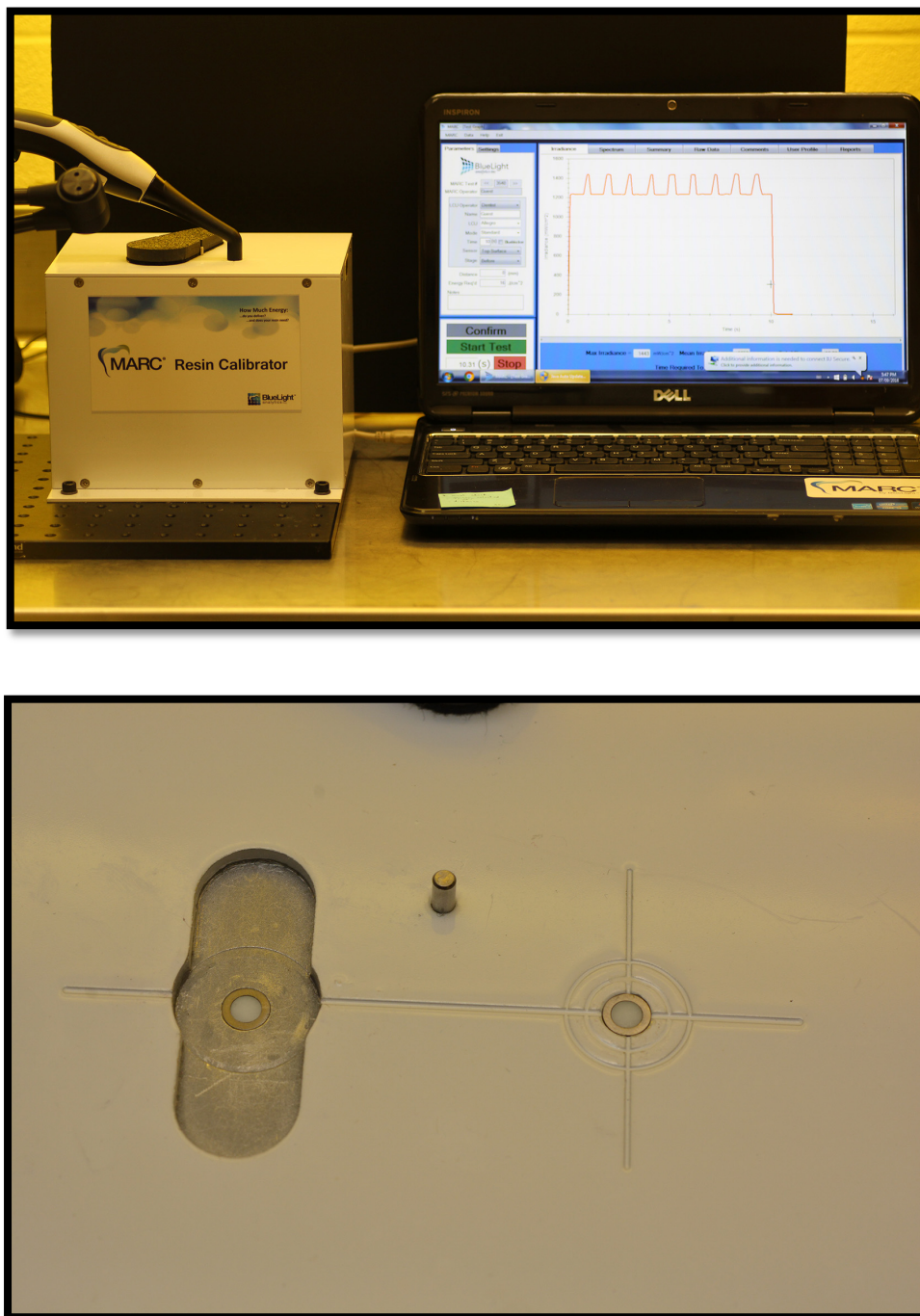


FIGURE 2. Top: A Managing Accurate Resin Curing System-Resin Calibrator (MARC-RC) system. Bottom: MARC-RC top sensor (right) and bottom sensor (left).

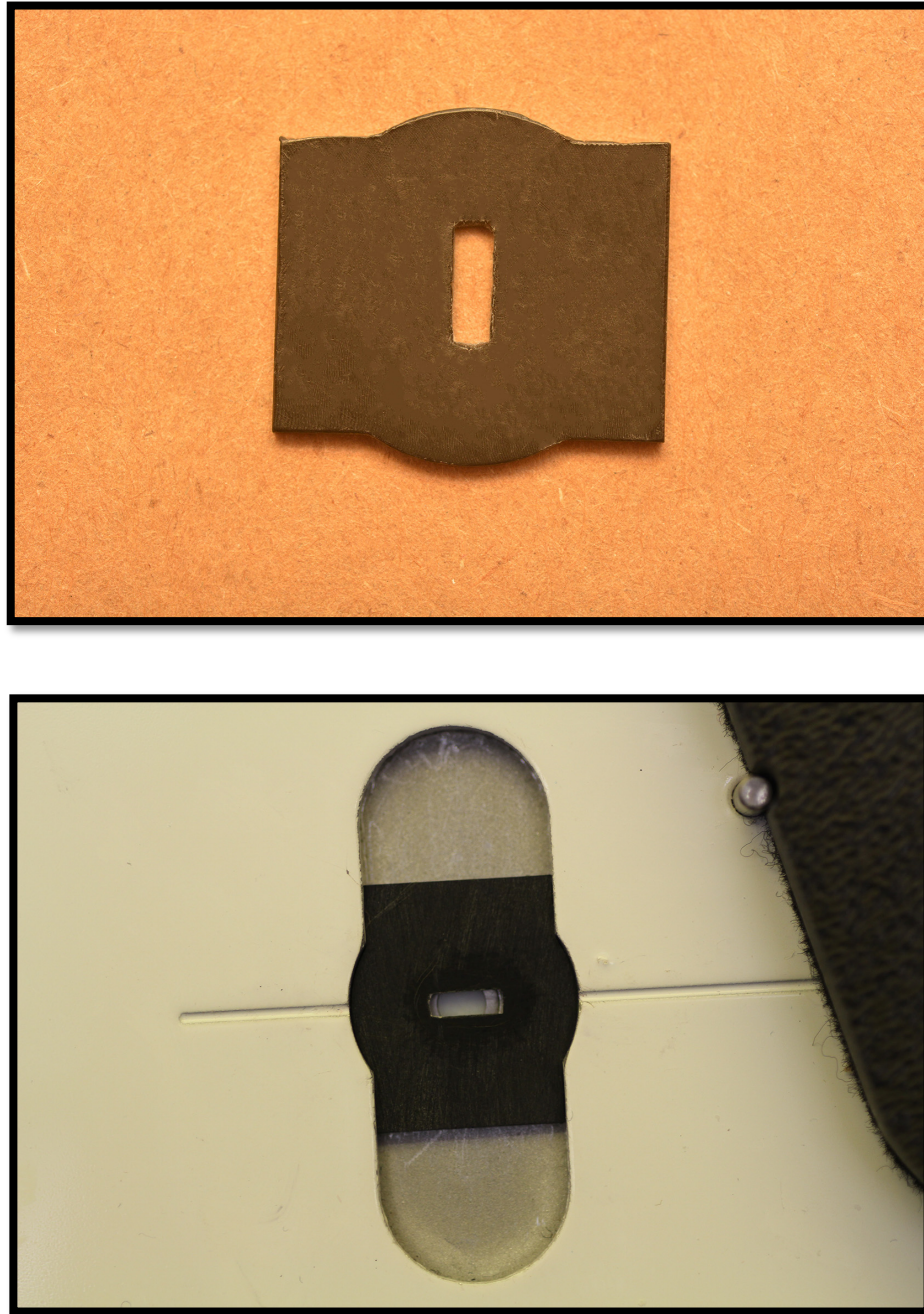


FIGURE 3. Top: Polyvinyl chloride (PVC) dark mold that has a rectangular opening with dimensions of (2mm width  $\times$  1 mm thickness  $\times$  6mm length) to fabricate RMC specimens. Bottom: The rectangular opening of the PVC mold centered over the 4 mm MARC-RC bottom sensor.





FIGURE 4. Illustration of the RMC packed into the rectangular opening of the mold with a hand instrument.

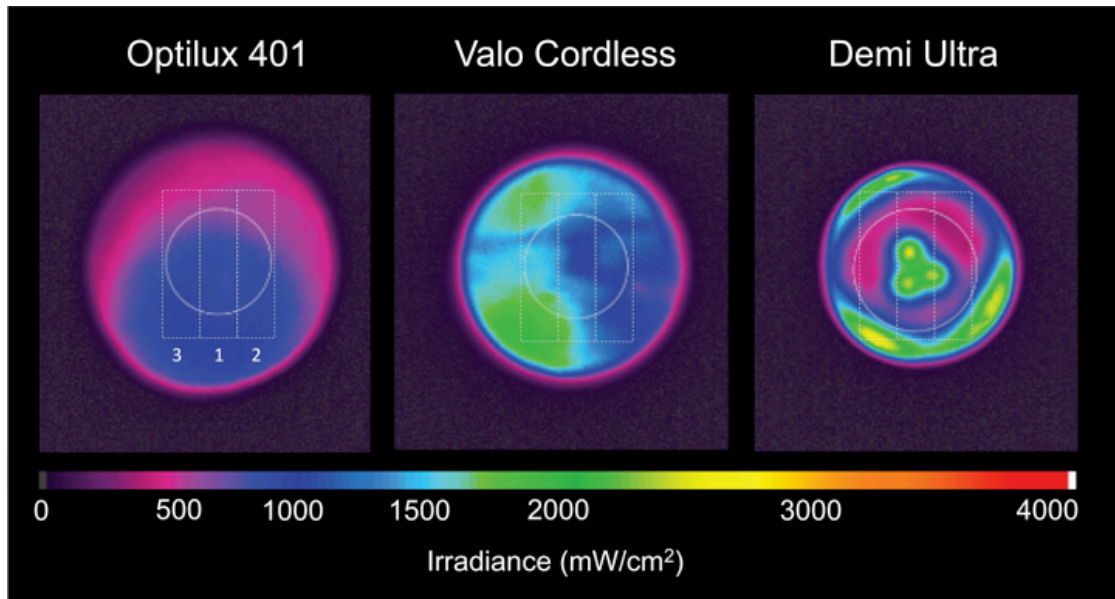


FIGURE 5. Illustration of the specimen locations where the measurements were collected relative to each light-curing unit (LCU) tip. The circle in the center of each image represents the 4-mm MARC-RC sensor where the irradiance measurements were collected. The dashed lines represent the light-curing unit locations where the light was irradiated and different measurements were collected. Numbers represent the specimen location. Abbreviations: Location 1: The center of the end of the tip. Location 2: LCU moved 1.5 mm to the left of the center of the end of the tip. Location 3: LCU moved 1.5 mm to the right of the center of the end of the tip.

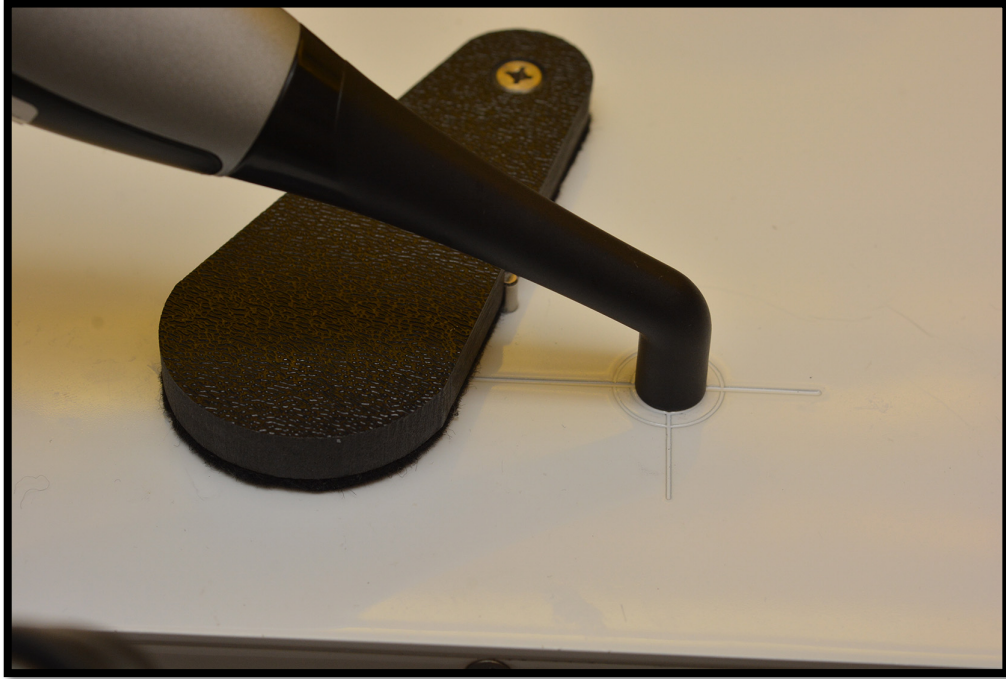


FIGURE 6. Illustration of the LED LCU mounted over the top sensor of MARC-RC to measure the amount of irradiance and radiant exposure received by the top surface of RMC specimen.



FIGURE 7. Illustration of the LED LCU mounted over the bottom sensor of MARC-RC and at 0-mm distance between the top of the specimen and the light guide to measure the amount of irradiance and radiant exposure received by the bottom surface of RMC specimen.



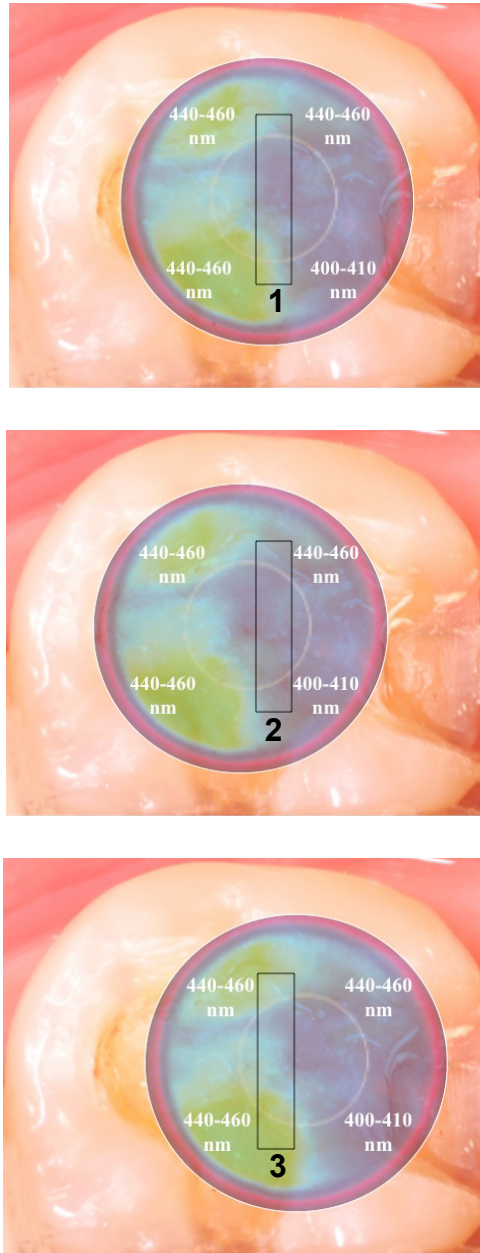


FIGURE 8. Illustration of the specimen locations relative to the beam profile of the LCU and superimposed over a Class II cavity preparation at different LCLs (1, 2, 3). Three irradiance hotspots deliver higher irradiance at spectral emission of 440 460 nm and one hotspot delivers lower irradiance at spectral emission of 400-410 nm. 1: The center of the end of the tip. Location 2: LCU moved 1.5 mm to the left of the center of the end of the tip. Location 3: LCU moved 1.5 mm to the right of the center of the end of the tip.

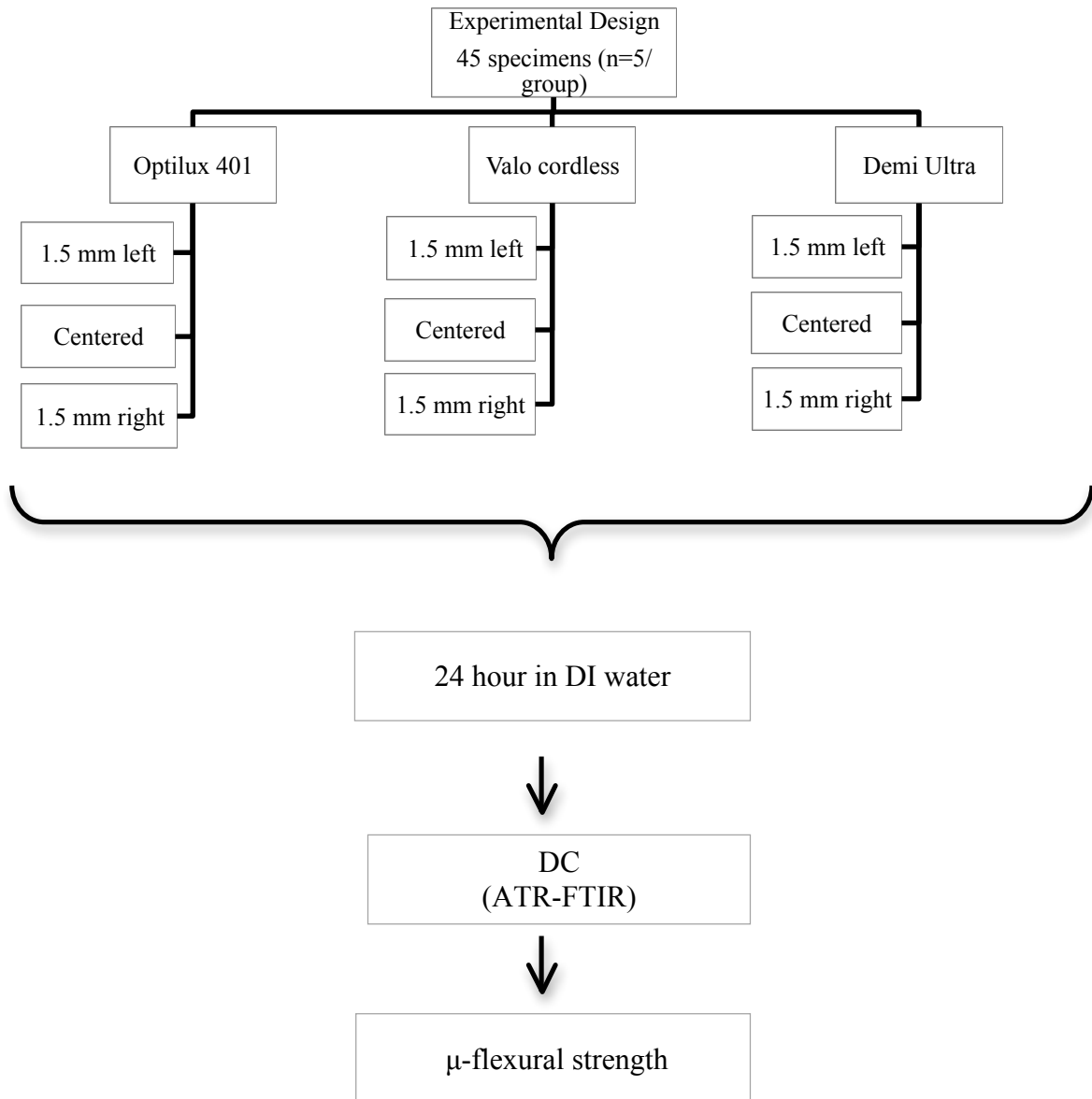


FIGURE 9. Flowchart of the experimental design. Abbreviations. DC: Degree of conversion.  $\mu$ -flexural strength: micro-flexural strength.

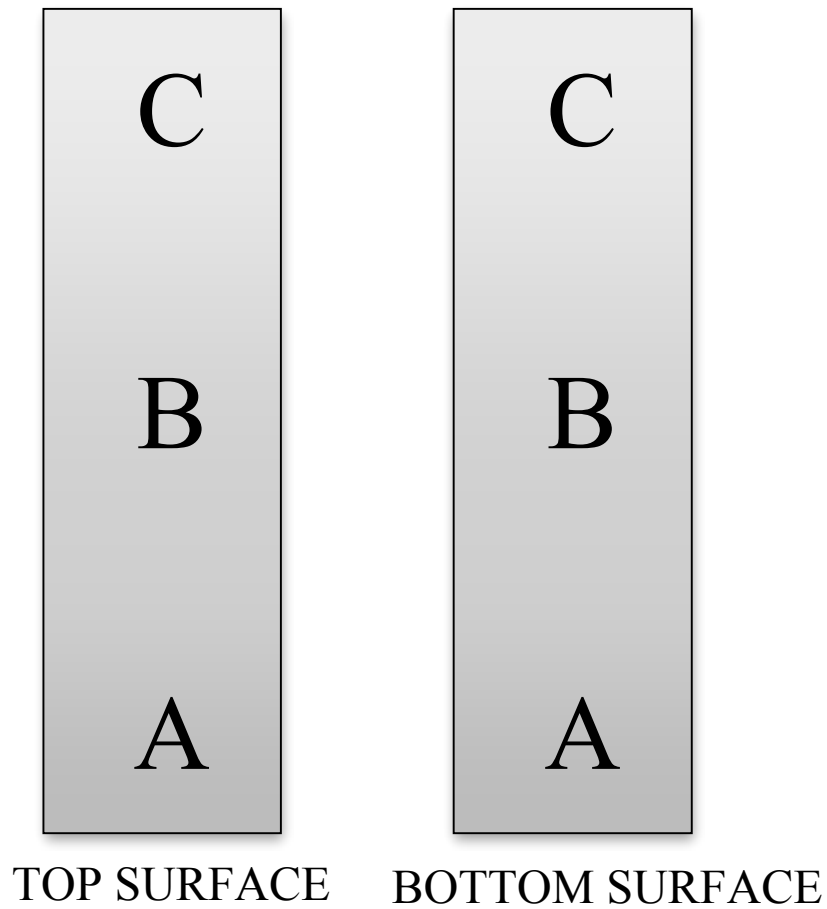


FIGURE 10. Illustration of the degree of conversion (DC) measurement locations on the top and bottom surfaces of a RMC specimen. A: DC measurement below the center of a RMC specimen. B: DC measurement at the center of a RMC specimen. C: DC measurement above the center of a RMC specimen.

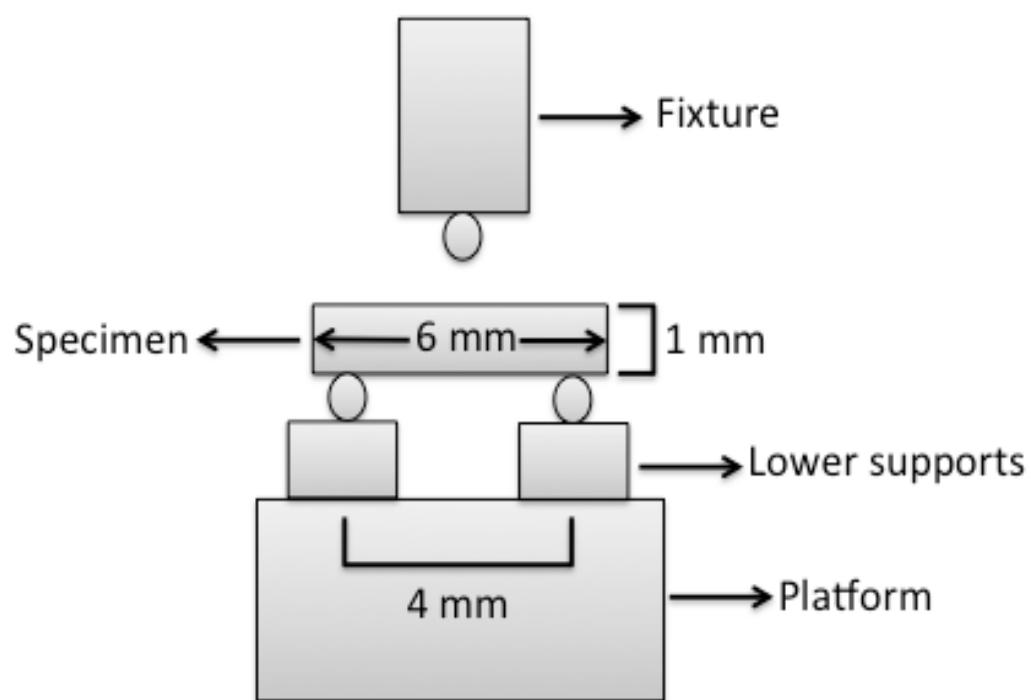


FIGURE 11. Illustration of  $\mu$ -flexural strength test setup.

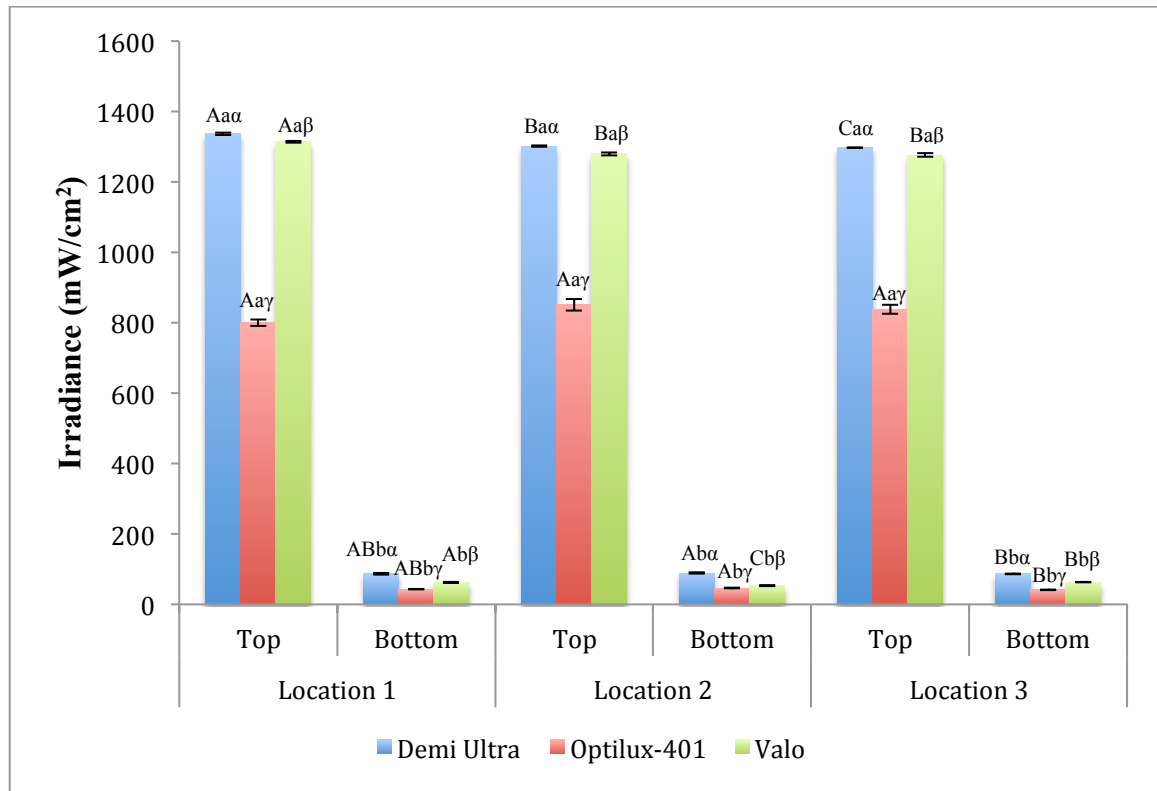


FIGURE 12. Mean  $\pm$ SE of the irradiance ( $\text{mW}/\text{cm}^2$ ) for the evaluated LCUs at different locations. Location 1: The center of the end of the tip. Location 2: LCU moved 1.5 mm to the left of the center of the end of the tip. Location 3: LCU moved 1.5 mm to the right of the center of the end of the tip. Uppercase letters represent statistical groups between locations for each LCU. Lowercase letters represent statistical groups between top and bottom surfaces. Greek letters represent statistical groups between LCUs.

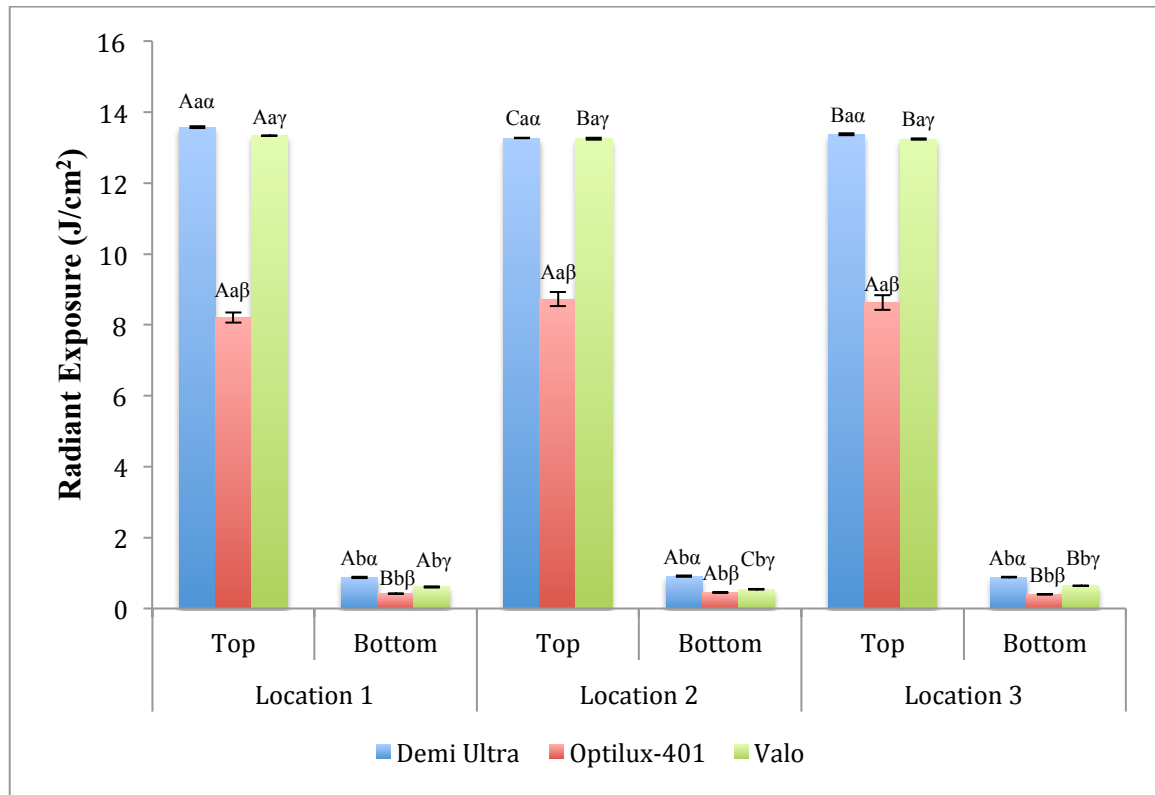


FIGURE 13. Mean  $\pm$ SE of the radiant exposure ( $\text{J}/\text{cm}^2$ ) for the evaluated LCUs at different locations. Location 1: The center of the end of the tip. Location 2: LCU moved 1.5 mm to the left of the center of the end of the tip. Location 3: LCU moved 1.5 mm to the right of the center of the end of the tip. Uppercase letters represent statistical groups between locations for each LCU. Lowercase letters represent statistical groups between top and bottom surfaces. Greek letters represent statistical groups between LCUs.

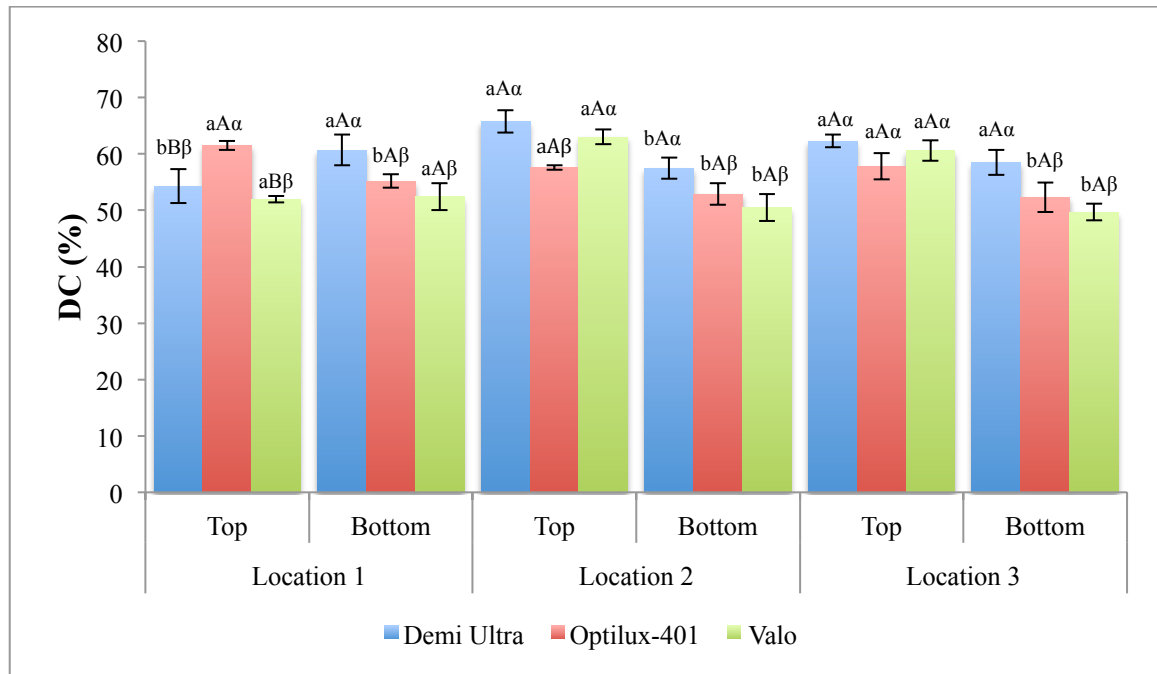


FIGURE 14. Mean  $\pm$ SE of DC for the evaluated LCUs at different locations. Location 1: The center of the end of the tip. Location 2: LCU moved 1.5 mm to the left of the center of the end of the tip. Location 3: LCU moved 1.5 mm to the right of the center of the end of the tip. Lowercase letters represent statistical groups between top and bottom surfaces for each LCU. Uppercase letters represent statistical groups between locations for each LCU. Greek letters represent statistical groups between LCUs for each surface.

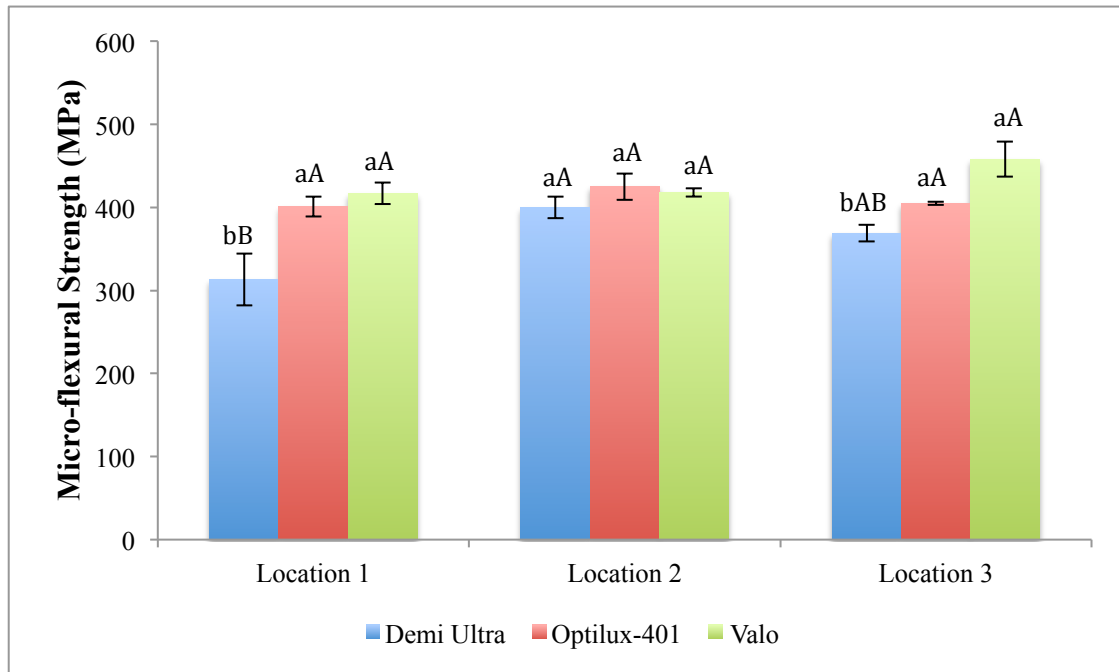


FIGURE 15. Mean  $\pm$ SE of  $\mu$ -flexural strength (MPa) for the evaluated LCUs at different locations. Location 1: The center of the end of the tip. Location 2: LCU moved 1.5 mm to the left of the center of the end of the tip. Location 3: LCU moved 1.5 mm to the right of the center of the end of the tip. Lowercase letters represent statistical groups between LCUs within the same location. Uppercase letters represent statistical groups between locations for each LCU.



## DISCUSSION

## IRRADIANCE AND RADIANT EXPOSURE

The ISO 4049 Standard for flexural strength<sup>71</sup> test suggests specimen dimensions of 2-mm width  $\times$  2-mm thickness  $\times$  25-mm length. However, specimens of this size require multiple overlapping irradiation cycles. Therefore, in this study, to assess the effect of non-uniform polymerization of RMC, a micro-flexural strength test was used. However there is no ISO standard for specimen dimensions of the micro-flexural strength test.<sup>33,35,37,72,73</sup> Also, the 16:1 proportion of the span to depth ratio that was suggested to minimize shear and local deformation effects was impractical and could not be used in this study, as the specimens became very thin and more prone to fracture during preparation.<sup>35</sup> Therefore, the dimensions were modified to 2-mm width  $\times$  1-mm thickness  $\times$  6-mm length to allow the light guide to completely cover the sample length, thereby curing samples in a single exposure.

For each LCU, it is important to note that the irradiance was collected from the 4-mm MARC-RC cosine corrector, which does not represent the effective light-emitting portion of the LCU tip. The significant differences observed between the LCL may be attributed to the differences in the beam profile radiated from each LCU. Also, RMC specimens cured at 0-mm distance from the LCU tip may not represent an actual clinical scenario and may receive higher irradiance and radiant exposure on the top and bottom surfaces.

Figure 2 shows higher irradiance at the center of the LCU tip for both DU and V. DU decreased on either side of the LCU, while V decreased only on the right side of the center. That could explain the significantly higher irradiance and radiant exposure delivered to the top surface at LCL 1 compared with LCLs 2 and 3 using DU and bottom at LCL 1 compared with LCL 2 using V. In addition, it could also explain the significantly lower irradiance and radiant exposure observed on the bottom at LCL 2 compared with LCL 3 using V. However, the presence of the LED violet chip in the lower right side of the multiple emission peak LED LCU tip may explain the lower irradiance and radiant exposure values on bottom surfaces at LCL 2. Although the irradiance is higher to the left of the center of the light curing unit tip in V, the significantly higher irradiance and radiant exposure at LCL 1 compared with LCL 3 on the top could be related to the convexity of the tip, which may focus the irradiance at the center of the light guide tip. Also, the higher irradiance delivered at LCL 2 compared with LCL 3 on the top and bottom using DU could be attributed to the larger area of high irradiance that covered the specimens at LCL 2. Although significantly lower radiant exposure was delivered on the top using DU at LCL 2 and 3, these differences may not be clinically significant. Even though O had relatively the most uniform light beam profile, the slight differences in the irradiance across the light beam profile could explain the significant differences observed in irradiance and radiant exposure on the bottom surfaces of RMC specimens.

#### DEGREE OF CONVERSION (DC)

Polymerization of RMC is mainly dependent on the curing conditions and material composition, which may affect their mechanical properties.<sup>74-77</sup> One of the

factors that affect the polymerization of a RMC is the photoinitiator system. CQ is the most common photoinitiator used in RMC.<sup>78</sup> Alternative photoinitiators, such as TPO, were introduced to overcome the yellow color of CQ.<sup>26,79,80</sup> As a result, multiple emission peak LED LCUs, which include an additional peak within the absorption range of TPO (350 nm to 425 nm) were developed.<sup>81</sup> Multiple emission peak blue-violet LED LCUs contain blue and violet chips, with spectral emission peaks of 440 nm to 460 nm and 400 nm to 410 nm, respectively, which have been suggested to improve the polymerization of TPO-containing RMC.<sup>26,82,83</sup> The RMC used in this study contains the TPO photoinitiator system, which may have different polymerization behavior than CQ and could result in higher polymerization rates compared with non-TPO RMC.<sup>84</sup> However, the bleaching shade used in the present study may improve the light transmission through the specimens and consequently result in higher DC values compared with darker shades.<sup>85,86</sup> On the other hand, the thickness of the specimens (1 mm) used in the present study may allow more light transmission through the material and result in higher DC values on bottom surfaces of specimens compared with the maximum thickness (2 mm) suggested for each RMC increment.<sup>87,88</sup>

Pigments and photoinitiators may decrease the amount of the light transmitted through RMC restorations; this may explain the same or significantly lower DC on the bottom of a specimen compared with the top.<sup>85,86</sup> However, the significantly higher DC on the bottom compared with the top using DU at LCL 1 may be explained by the light reflected off the radiopaque MARC-RC bottom sensor to the bottom surfaces.

The lower DC values with DU on the T at LCL 1 compared to LCL 2 and 3 could be related to the high amount of free radicals produced from RMC specimens, which may

result in higher rate of polymerization that rapidly increased the viscosity of the dimethacrylate monomer system and consequently restricted the mobility of the molecules, resulting in more free radical entrapment, increased termination, and lower DC values.<sup>38</sup> In addition, the lower DC values with V on the top at LCL 1 compared with LCL 2 and 3 could be related to the presence of the LED violet chip at LCL 2.<sup>19, 26-28</sup>

The significantly higher DC values of DU compared to O and V on the bottom at all LCLs can be attributed to the higher irradiance and radiant exposure delivered with DU. This result confirms previous findings on the correlation of irradiance and radiant exposure with DC.<sup>32, 54</sup> Also, the higher DC on the top using O compared with DU and V at LCL 1 could be related to the broad spectral emission and uniform light beam profile of O LCU. However, the higher DC on the top using DU and V compared with O at LCL 2 could be attributed to the high irradiance and radiant exposure delivered by DU and V compared with O.<sup>32,54</sup>

#### MICRO-FLEXURAL STRENGTH ( $\mu$ -flexural strength)

The monomer concentration, viscosity, and inorganic filler morphology may also affect the DC and flexural strength of RMC, which vary among different types of RMC.<sup>56-59</sup> The significantly lower  $\mu$ -flexural strength using DU at LCL 1 than 2 may be related to the rate of polymerization, as the TPO may not be efficiently activated because higher irradiance was delivered to the sample within the CQ range and not the TPO range (violet range) and could result in lower cross linked density, which could influence the mechanical properties of RMC.<sup>19,26-28,38</sup> These results may confirm the previous findings on the correlation between adequate polymerization and the  $\mu$ -flexural strength of RMC.<sup>31,32,54,55</sup> The significantly lower  $\mu$ -flexural strength for DU compared with O and V

at LCL 1 and 3 could be related to the broad spectral emission of O and V LCUs because a QTH LCU has a more uniform light beam profile than LED LCUs, which were reported to be non-uniform.<sup>20,46</sup>

Among the limitations of this study, only one type of RMC was analyzed. Therefore, due to the large diversity of RMC products, it might be difficult to generalize the results of this study to other RMCs. Instead, our results may provide a reference about the possible impact of light beam profile non-uniformity on the polymerization and mechanical properties of RMC materials.

The findings of this study demonstrated significant variations in the DC and flexural strength of a RMC. Therefore, more studies are needed to further investigate and understand this possible detrimental effect. Furthermore, besides the importance of optimizing the exposure time and distance between the LCU tip and RMC restoration, clinicians should consider the type of photoinitiators used in RMC relative to the spectral emission of various types of LCUs present in the market.

Future studies should continue to evaluate the effect of light beam non-uniformity of different LED LCUs on the mechanical properties of RMC cured at several distances from LCU tip and with various exposure times and photoinitiator systems. Also, future work should examine the variation of DC by mapping DC values across the top and bottom surfaces of RMC specimens to provide an accurate representation on the effect of the light beam non-uniformity on the polymerization of RMC restorations.

## SUMMARY AND CONCLUSIONS

This study showed that bottom surfaces of RMC specimens received significantly lower irradiance and radiant exposure than top surfaces irrespective of LCL or LCU. All LCUs exhibited significant differences in the DC values between top and bottom surfaces at all LCLs except for V LCL 1 and DU LCL 3. Also, DU and V showed lower DC values on top surfaces at LCL 1 than 2 and 3. The  $\mu$ -flexural strength was significantly lower for DU LED LCU at LCL 1 than LCL 2. Therefore, the non-uniform light curing beam profile could have a significant effect on  $\mu$ -flexural strength and DC of RMC specimens cured at different LCLs.



## REFERENCES

1. Heintze SD, Rousson V. Clinical effectiveness of direct class II restorations - a meta-analysis. *J Adhes Dent* 2012;14(5):407-31.
2. Rasines Alcaraz MG, Veitz-Keenan A, Sahrmann P, et al. Direct composite resin fillings versus amalgam fillings for permanent or adult posterior teeth. *Cochrane Database Syst Rev* 2014;3:CD005620.
3. Kopperud SE, Tveit AB, Gaarden T, Sandvik L, Espelid I. Longevity of posterior dental restorations and reasons for failure. *Eur J Oral Sci* 2012;120(6):539-48.
4. Sunnegardh-Gronberg K, van Dijken JW, Funegard U, Lindberg A, Nilsson M. Selection of dental materials and longevity of replaced restorations in Public Dental Health clinics in northern Sweden. *J Dent* 2009;37(9):673-8.
5. Rho YJ, Namgung C, Jin BH, Lim BS, Cho BH. Longevity of direct restorations in stress-bearing posterior cavities: a retrospective study. *Oper Dent* 2013;38(6):572-82.
6. Opdam NJ, Bronkhorst EM, Roeters JM, Loomans BA. A retrospective clinical study on longevity of posterior composite and amalgam restorations. *Dent Mater* 2007;23(1):2-8.
7. Bernardo M, Luis H, Martin MD, et al. Survival and reasons for failure of amalgam versus composite posterior restorations placed in a randomized clinical trial. *J Am Dent Assoc* 2007;138(6):775-83.
8. Calheiros FC, Daronch M, Rueggeberg FA, Braga RR. Influence of irradiant energy on degree of conversion, polymerization rate and shrinkage stress in an experimental resin composite system. *Dent Mater* 2008;24(9):1164-8.
9. Arikawa H, Kanie T, Fujii K, Shinohara N. Bending strength and depth of cure of light-cured composite resins irradiated using filters that simulate enamel. *J Oral Rehabil* 2004;31(1):74-80.
10. Lovell LG, Newman SM, Bowman CN. The effects of light intensity, temperature, and comonomer composition on the polymerization behavior of dimethacrylate dental resins. *J Dent Res* 1999;78(8):1469-76.
11. Price RB, Ferracane JL, Shortall AC. Light-curing units: a review of what we need to know. *J Dent Res* 2015;94(9):1179-86.

12. Barghi N, Fischer DE, Pham T. Revisiting the intensity output of curing lights in private dental offices. *Compend Contin Educ Dent* 2007;28(7):380-4; quiz 85-6.
13. Al Shaafi M, Maawadh A, Al Qahtani M. Evaluation of light intensity output of QTH and LED curing devices in various governmental health institutions. *Oper Dent* 2011;36(4):356-61.
14. Maghaireh GA, Alzraikat H, Taha NA. Assessing the irradiance delivered from light-curing units in private dental offices in Jordan. *J Am Dent Assoc* 2013;144(8):922-7.
15. Arikawa H, Kanie T, Fujii K, Takahashi H, Ban S. Effect of inhomogeneity of light from light curing units on the surface hardness of composite resin. *Dent Mater J* 2008;27(1):21-8.
16. Michaud PL, Price RB, Labrie D, Rueggeberg FA, Sullivan B. Localised irradiance distribution found in dental light curing units. *J Dent* 2014;42(2):129-39.
17. Price RB, Labrie D, Rueggeberg FA, et al. Correlation between the beam profile from a curing light and the microhardness of four resins. *Dent Mater* 2014;30(12):1345-57.
18. Vandewalle KS, Roberts HW, Rueggeberg FA. Power distribution across the face of different light guides and its effect on composite surface microhardness. *J Esthet Restor Dent* 2008;20(2):108-17; discussion 18.
19. Price RB, Labrie D, Whalen JM, Felix CM. Effect of distance on irradiance and beam homogeneity from 4 light-emitting diode curing units. *J Can Dent Assoc* 2011;77:b9.
20. Megremis SJ, Ong V, Lukic H, Shepelak H. An ada laboratory evaluation of light-emitting diode curing units. *J Am Dent Assoc* 2014;145(11):1164-6.
21. Price RB, Labrie D, Rueggeberg FA, Felix CM. Irradiance differences in the violet (405 nm) and blue (460 nm) spectral ranges among dental light-curing units. *J Esthet Restor Dent* 2010;22(6):363-77.
22. Durner J, Obermaier J, Draenert M, Ilie N. Correlation of the degree of conversion with the amount of elutable substances in nano-hybrid dental composites. *Dent Mater* 2012;28(11):1146-53.
23. Haenel T, Hausnerova B, Steinhaus J, et al. Effect of the irradiance distribution from light curing units on the local micro-hardness of the surface of dental resins. *Dent Mater* 2015;31(2):93-104.

24. Ferracane JL, Mitchem JC, Condon JR, Todd R. Wear and marginal breakdown of composites with various degrees of cure. *J Dent Res* 1997;76(8):1508-16.
25. Watts DC. Reaction kinetics and mechanics in photo-polymerised networks. *Dent Mater* 2005;21(1):27-35.
26. Rueggeberg FA. State-of-the-art: dental photocuring--a review. *Dent Mater* 2011;27(1):39-52.
27. Nomoto R. Effect of light wavelength on polymerization of light-cured resins. *Dent Mater J* 1997;16(1):60-73.
28. Price RB, Felix CA. Effect of delivering light in specific narrow bandwidths from 394 to 515nm on the micro-hardness of resin composites. *Dent Mater* 2009;25(7):899-908.
29. Craig RG, editor. *Restorative dental materials*. St. Louis: Mosby; 1997.
30. Reinhardt JW, Boyer DB, Stephens NH. Effects of secondary curing on indirect posterior composite resins. *Oper Dent* 1994;19(6):217-20.
31. Palin WM, Fleming GJ, Burke FJ, Marquis PM, Randall RC. Monomer conversion versus flexure strength of a novel dental composite. *J Dent* 2003;31(5):341-51.
32. Calheiros FC, Kawano Y, Stansbury JW, Braga RR. Influence of radiant exposure on contraction stress, degree of conversion and mechanical properties of resin composites. *Dent Mater* 2006;22(9):799-803.
33. Munchow EA, Zanchi CH, Ogliari FA, et al. Replacing HEMA with alternative dimethacrylates in dental adhesive systems: evaluation of polymerization kinetics and physicochemical properties. *J Adhes Dent* 2014;16(3):221-8.
34. Lúcia Rodrigues Macedo C, Aldrighi Münchow E, da Silveira Lima G, et al. Incorporation of inorganic fillers into experimental resin adhesives: Effects on physical properties and bond strength to dentin. *Int J Adhes Adhesives* 2015;62:78-84.
35. Chiaraputt S, Mai S, Huffman BP, et al. Changes in resin-infiltrated dentin stiffness after water storage. *J Dent Res* 2008;87(7):655-60.
36. Czasch P, Ilie N. In vitro comparison of mechanical properties and degree of cure of bulk fill composites. *Clin Oral Investig* 2013;17(1):227-35.
37. Ilie N, Bauer H, Draenert M, Hickel R. Resin-based composite light-cured properties assessed by laboratory standards and simulated clinical conditions. *Oper Dent* 2013;38(2):159-67.

38. Leprince JG, Palin WM, Hadis MA, Devaux J, Leloup G. Progress in dimethacrylate-based dental composite technology and curing efficiency. *Dent Mater* 2013;29(2):139-56.
39. Main C, Cummings A, Moseley H, Stephen KW, Gillespie FC. An assessment of new dental ultraviolet sources and u.v.-polymerized fissure sealants. *J Oral Rehabil* 1983;10(3):215-27.
40. Moseley H, Strang R, Stephen KW. An assessment of visible-light polymerizing sources. *J Oral Rehabil* 1986;13(3):215-24.
41. Craig R. Chemistry composition, and properties of composite resins. In: Horn H, editor. *Symposium on composite resins in dentistry*. Philadelphia, Saunders: The Dental Clinics of North America; 1981. p. 219–39
42. Neo JC, Denehy GE, Boyer DB. Effects of polymerization techniques on uniformity of cure of large-diameter, photo-initiated composite resin restorations. *J Am Dent Assoc* 1986;113(6):905-9.
43. Spectral curing lights and evolving technology. ADA professional product review. Chicago (IL): American Dental Association; 2009. pp. 1–16.
44. Vandewalle KS, Roberts HW, Andrus JL, Dunn WJ. Effect of light dispersion of LED curing lights on resin composite polymerization. *J Esthet Restor Dent* 2005;17(4):244-54; discussion 54-5.
45. LBA-USB User Guide. Logan (UT): Ophir-Spiricon; 2006. pp. 100–2.
46. Price RB, Rueggeberg FA, Labrie D, Felix CM. Irradiance uniformity and distribution from dental light curing units. *J Esthet Restor Dent* 2010;22(2):86-101.
47. Leprince JG, Hadis M, Shortall AC, et al. Photoinitiator type and applicability of exposure reciprocity law in filled and unfilled photoactive resins. *Dent Mater* 2011;27(2):157-64.
48. Peutzfeldt A, Asmussen E. Resin composite properties and energy density of light cure. *J Dent Res* 2005;84(7):659-62.
49. Musanje L, Darvell BW. Polymerization of resin composite restorative materials: exposure reciprocity. *Dent Mater* 2003;19(6):531-41.
50. Shortall A, El-Mahy W, Stewardson D, Addison O, Palin W. Initial fracture resistance and curing temperature rise of ten contemporary resin-based composites with increasing radiant exposure. *J Dent* 2013;41(5):455-63.

51. Bayne SC. Correlation of clinical performance with 'in vitro tests' of restorative dental materials that use polymer-based matrices. *Dent Mater* 2012;28(1):52-71.
52. Shortall AC, Felix CJ, Watts DC. Robust spectrometer-based methods for characterizing radiant exitance of dental LED light curing units. *Dent Mater* 2015;31(4):339-50.
53. Ferracane JL. Correlation between hardness and degree of conversion during the setting reaction of unfilled dental restorative resins. *Dent Mater* 1985;1(1):11-4.
54. Gonzalez MR, Poskus LT, Sampaio Filho HR, Perez CR. Influence of irradiance and exposure time on the degree of conversion and mechanical properties of a conventional and silorane composite. *Indian J Dent Res* 2013;24(6):719-22.
55. Lovell LG, Lu H, Elliott JE, Stansbury JW, Bowman CN. The effect of cure rate on the mechanical properties of dental resins. *Dent Mater* 2001;17(6):504-11.
56. Amirouche-Korichi A, Mouzali M, Watts DC. Effects of monomer ratios and highly radiopaque fillers on degree of conversion and shrinkage-strain of dental resin composites. *Dent Mater* 2009;25(11):1411-8.
57. Sideridou I, Tserki V, Papanastasiou G. Effect of chemical structure on degree of conversion in light-cured dimethacrylate-based dental resins. *Biomaterials* 2002;23(8):1819-29.
58. Goncalves F, Kawano Y, Pfeifer C, Stansbury JW, Braga RR. Influence of BisGMA, TEGDMA, and BisEMA contents on viscosity, conversion, and flexural strength of experimental resins and composites. *Eur J Oral Sci* 2009;117(4):442-6.
59. Kim KH, Ong JL, Okuno O. The effect of filler loading and morphology on the mechanical properties of contemporary composites. *J Prosthet Dent* 2002;87(6):642-9.
60. Cowie JMG. *Polymers: chemistry and physics of modern materials*. 2nd ed. Glasgow, New York: Blackie, Chapman and Hall; 1991.
61. Callister WD, Callister WD. *Fundamentals of materials science and engineering : an interactive etext*. New York: Wiley; 2001.
62. Freilich MA, Karmaker AC, Burstone CJ, Goldberg AJ. Development and clinical applications of a light-polymerized fiber-reinforced composite. *J Prosthet Dent* 1998;80(3):311-8.
63. Vallittu PK, Sevelius C. Resin-bonded, glass fiber-reinforced composite fixed partial dentures: a clinical study. *J Prosthet Dent* 2000;84(4):413-8.

64. Bae JM, Kim KN, Hattori M, et al. Fatigue strengths of particulate filler composites reinforced with fibers. *Dent Mater J* 2004;23(2):166-74.
65. Nielsen LE. Mechanical properties of polymer and composites. New York: Marcel Dekker Inc; 1974 p. 468–88.
66. Dyer SR, Lassila LV, Jokinen M, Vallittu PK. Effect of fiber position and orientation on fracture load of fiber-reinforced composite. *Dent Mater* 2004;20(10):947-55.
67. <http://curingresin.com/wp-content/uploads/2012/08/MARC-RC-Brochure-v4.2.pdf>; 2014.
68. Bucuta S, Ilie N. Light transmittance and micro-mechanical properties of bulk fill vs. conventional resin based composites. *Clin Oral Investig* 2014;18(8):1991-2000.
69. A.O. Al-Zain, Ph.D. dissertation, June 2015.
70. Albino LG, Rodrigues JA, Kawano Y, Cassoni A. Knoop microhardness and FT-Raman evaluation of composite resins: influence of opacity and photoactivation source. *Braz Oral Res* 2011;25(3):267-73.
71. Standardization(ISO) IOF. ISO-4049 Dentistry- Polymer- based restorative materials. Flexural strength; 2009.
72. Calheiros FC, Pfeifer CS, Brandao LL, Agra CM, Ballester RY. Flexural properties of resin composites: influence of specimen dimensions and storage conditions. *Dent Mater J* 2013;32(2):228-32.
73. Peutzfeldt A, Asmussen E. Mechanical properties of three composite resins for the inlay/onlay technique. *J Prosthet Dent* 1991;66(3):322-4.
74. Santos GB, Medeiros IS, Fellows CE, Muench A, Braga RR. Composite depth of cure obtained with QTH and LED units assessed by microhardness and micro-Raman spectroscopy. *Oper Dent* 2007;32(1):79-83.
75. Miletic VJ, Santini A. Remaining unreacted methacrylate groups in resin-based composite with respect to sample preparation and storing conditions using micro-Raman spectroscopy. *J Biomed Mater Res B Appl Biomater* 2008;87(2):468-74.
76. Tarle Z, Knezevic A, Demoli N, et al. Comparison of composite curing parameters: effects of light source and curing mode on conversion, temperature rise and polymerization shrinkage. *Oper Dent* 2006;31(2):219-26.

77. Knezevic A, Tarle Z, Meniga A, et al. Degree of conversion and temperature rise during polymerization of composite resin samples with blue diodes. *J Oral Rehabil* 2001;28(6):586-91.
78. Stansbury JW. Curing dental resins and composites by photopolymerization. *J Esthet Dent* 2000;12(6):300-8.
79. Neumann MG, Miranda WG, Jr., Schmitt CC, Rueggeberg FA, Correa IC. Molar extinction coefficients and the photon absorption efficiency of dental photoinitiators and light curing units. *J Dent* 2005;33(6):525-32.
80. Palin WM, Senyilmaz DP, Marquis PM, Shortall AC. Cure width potential for MOD resin composite molar restorations. *Dent Mater* 2008;24(8):1083-94.
81. Santini A. Current status of visible light activation units and the curing of light-activated resin-based composite materials. *Dent Update* 2010;37(4):214-6, 18-20, 23-7.
82. Jandt KD, Mills RW. A brief history of LED photopolymerization. *Dent Mater* 2013;29(6):605-17.
83. Arikawa H, Takahashi H, Kanie T, Ban S. Effect of various visible light photoinitiators on the polymerization and color of light-activated resins. *Dent Mater J* 2009;28(4):454-60.
84. Schneider LF, Cavalcante LM, Pahl SA, Pfeifer CS, Ferracane JL. Curing efficiency of dental resin composites formulated with camphorquinone or trimethylbenzoyl-diphenyl-phosphine oxide. *Dent Mater* 2012;28(4):392-7.
85. Ogunyinka A, Palin WM, Shortall AC, Marquis PM. Photoinitiation chemistry affects light transmission and degree of conversion of curing experimental dental resin composites. *Dent Mater* 2007;23(7):807-13.
86. Musanje L, Darvell BW. Curing-light attenuation in filled-resin restorative materials. *Dent Mater* 2006;22(9):804-17.
87. Garoushi S, Vallittu P, Shinya A, Lassila L. Influence of increment thickness on light transmission, degree of conversion and micro hardness of bulk fill composites. *Odontology* 2015.
88. Sakaguchi RL, Douglas WH, Peters MC. Curing light performance and polymerization of composite restorative materials. *J Dent* 1992;20(3):183-8.



## ABSTRACT

INFLUENCE OF CURING-LIGHT BEAM PROFILE NON-UNIFORMITY ON  
DEGREE OF CONVERSION AND MICRO-FLEXURAL STRENGTH  
OF RESIN-MATRIX COMPOSITE

by

Yousef Tariq Eshmawi

Indiana University School of Dentistry  
Indianapolis, Indiana

Background. Beam profile non-uniformity of light-curing units (LCUs) may result in suboptimal properties of resin-matrix composite (RMC) restorations. Objectives: The objective of this study was to evaluate the effect of curing-light beam profile of multiple light curing units (LCUs) on the degree of conversion (DC) and micro-flexural strength ( $\mu$ -flexural strength) of RMC. Methods: Forty-five nano-filled hybrid RMC (Tetric EvoCeram, Ivoclar Vivadent, Amherst, NY) specimens were fabricated. Quartz-tungsten-halogen (QTH) (Optilux 401) (O), multiple emission peak (VALO Cordless) (V) and single emission peak (Demi Ultra) (DU) light-emitting-diode (LED) LCUs were

investigated at different light-curing locations (LCLs): 1) the center of the LCU tip; 2) 1.5 mm to the left of the center of the LCU tip; and 3) 1.5 mm to the right of the center of the LCU tip. Specimens were stored wet in deionized water at 37°C for 24 hours. The DC was measured on top and bottom surfaces using Attenuated Total Reflectance-Fourier Transform Infrared (ATR-FTIR) spectroscopy. Micro-flexural strength testing was performed using a universal mechanical testing machine at crosshead speed of 1 mm/min. Multi-factorial ANOVAs were used to analyze the data ( $\alpha = 0.05$ ). Results: All LCUs exhibited significant differences in DC between top and bottom surfaces at the different LCLs (Table I). Micro-flexural strength varied with LCL for DU (Table II). Conclusions: The non-uniform curing-light beam profile could have a significant effect on  $\mu$ -flexural strength and DC on top and bottom surfaces of RMC specimens cured at different LCLs. Key words. LED, QTH, Mechanical properties.

## CURRICULUM VITAE

## Yousef Tariq Eshmawi

2004 to 2010	Bachelor's Degree of Oral and Dental Medicine and Surgery. Misr University For Science and Technology, 6 <sup>th</sup> of October City, Cairo, Egypt.
2011 to 2012	One-year internship program,.King Abdulaziz University Faculty of Dentistry, Jeddah, Saudi Arabia.
2014 to 2017	Master of Science in Dentistry (M.S.D). Major in Operative Dentistry, Minor in Dental Materials and Preventive Dentistry. Certificate in Operative Dentistry. IUSD, Indianapolis, IN.

## Professional Organizations

International/American Association for Dental Research (IADR/AADR)  
The American Dental Education Association (ADEA)  
The Indiana Section of the American Association for Dental Research (IN-AADR)  
The Academy of Operative Dentistry (AOD)  
The Saudi Commission for Health Specialties